

## LA-UR-14-24979

Approved for public release; distribution is unlimited.

Title: Correlated Neutron and Gamma-Ray Emissions in MCNP6

Author(s): Rising, Michael E.  
Talou, Patrick  
Sood, Avneet  
Stetcu, Ionel  
Kawano, Toshihiko

Intended for: 2014 ANS Winter Meeting and Nuclear Technology Expo,  
2014-11-09/2014-11-13 (Anaheim, California, United States)

Issued: 2014-08-25 (rev.2)

---

**Disclaimer:**

Los Alamos National Laboratory, an affirmative action/equal opportunity employer, is operated by the Los Alamos National Security, LLC for the National Nuclear Security Administration of the U.S. Department of Energy under contract DE-AC52-06NA25396. By approving this article, the publisher recognizes that the U.S. Government retains nonexclusive, royalty-free license to publish or reproduce the published form of this contribution, or to allow others to do so, for U.S. Government purposes. Los Alamos National Laboratory requests that the publisher identify this article as work performed under the auspices of the U.S. Department of Energy. Los Alamos National Laboratory strongly supports academic freedom and a researcher's right to publish; as an institution, however, the Laboratory does not endorse the viewpoint of a publication or guarantee its technical correctness.

## Correlated Neutron and Gamma-Ray Emissions in MCNP6

Michael E. Rising, Avneet Sood, Patrick Talou, Ionel Stetcu, and Toshihiko Kawano

*Los Alamos National Laboratory, MS B283, Los Alamos, NM, 87545, USA*  
*mrising@lanl.gov, talou@lanl.gov, sooda@lanl.gov*

### INTRODUCTION

A predictive capability to model and design passive and active interrogation systems for special nuclear material (SNM) detection is of great importance to global security and for nuclear nonproliferation applications. One approach to solve some of these problems is to model passive or active interrogation designs in a transport code to predict if and what SNM signatures can be identified. Unfortunately, the set of tabulated data present in modern evaluated nuclear data libraries is limited to average quantities only, such as the average neutron multiplicity, or the average prompt fission neutron spectrum. Quantities such as the prompt neutron multiplicity distribution, or multiplicity-dependent prompt fission neutron spectra are not present. For example when the MCNP 6 [1] transport code is used for a neutron-photon problem in default mode, if a neutron has any kind of reaction (capture, inelastic scatter, fission, etc.) with a material in the problem that has a non-zero total photon production cross section then the emission photons are independently produced from a randomly sampled photon production cross section. This means that as the number of reactions increase the photons produced behave correctly on average, but for each individual event there is no correlation to the incident neutron reaction that actually occurred in the system. If we are to have a predictive capability in SNM signature detection, then modeling the specific emitted particles from fission events could help identify the presence and identity of fissile materials.

### BACKGROUND

The most recent version of MCNP 6.1.1 [2] contains two neutron-photon multiplicity packages: the LLNL Fission Library [3] which contains the Fission Reaction Event Yield Algorithm (FREYA) code [4] for correlated neutron-photon emissions from fission events and the Cascading Gamma-ray Multiplicity (CGM) code from LANL [5]. The CGM code handles a variety of reactions, but does not include emitted particles or photons from fission reactions. The upcoming release of a new code, CGMF, can be described as a superset of the original CGM code with the new capability of handling fission reactions. When the CGMF code is deemed ready for production, it will be implemented into MCNP 6 and made available in a future release.

### SECONDARY PARTICLE EVENT GENERATORS

The LANL CGMF code models the statistical nature of emitted particles from various reactions including spontaneous and neutron-induced fission events. In particular, CGMF performs event-by-event simulations of the decay of excited nuclei using the Hauser-Feshbach statistical theory of nuclear reactions [6]. Given a fission event occurs either spontaneously or by a neutron with incident energy on a target nucleus, CGMF statistically samples from a joint probability distribution of the mass ( $A$ ), charge ( $Z$ ) and total kinetic energy ( $TKE$ ) yields to obtain the initial conditions of the excited fission fragments. The spin and parity of the fission fragments are also determined and included in the initial conditions before the de-excitation of the fragments begins.

The Hauser-Feshbach statistical theory implemented in CGMF (and CGM) models the decay of a nucleus in an excited state as particles and photons are evaporated until the nuclei reaches a more stable state. Because the evaporation of the particles and photons is based on probabilities, the average quantities can be computed deterministically (which is a more traditional approach) while it is also possible to describe individual events or histories of the model using the Monte Carlo method. The latter method is preferred for this work because it maintains the correlations between the incident reaction and the secondary particles emitted and can be used as an event generator in the MCNP 6 transport code.

The FREYA code already implemented in MCNP 6 through the LLNL Fission Library package is similar to the CGMF code in that it acts as an event generator for neutron-induced and spontaneous fission events. One of the major differences between the two event generator codes is that FREYA uses a Monte Carlo Weisskopf approach while CGMF uses a Monte Carlo Hauser-Feshbach approach. The latter approach treats the competition between neutron and gamma-ray emission at each stage of the de-excitation of the fission fragments while the former approach emits neutrons only, sampled from a Weisskopf spectrum, until the residual excitation energy in the fission fragment falls below the yrast line. Then, after all neutrons have been emitted, the Monte Carlo Weisskopf approach in FREYA completes the calculation by emitting the gamma rays from the remainder of the residual energy. This difference in approach is noticeable in both the calculated results and the overall computation cost of the models [7]. While the

Monte Carlo Hauser-Feshbach is considered to be a more theoretically correct model, the Monte Carlo Weisskopf model is significantly faster in computational speed in comparison. When CGMF is finally integrated into MCNP 6, detailed comparisons with FREYA as well as with real-world SNM measurements will be necessary to validate the models and determine which performs best for various problems.

## NUMERICAL RESULTS

In the following, the MCNP 6 numerical results refer to the default behavior in which the reactions and secondary emissions are uncorrelated on an event-by-event basis and represent the total secondary particle emission from all reactions. The FREYA results refer to the LLNL Fission Library implementation in MCNP 6 meaning that the secondary particle emissions from fission events come from FREYA and are combined with all other secondary particle emissions, such as the  $(n,\gamma)$  capture reaction gamma-ray emissions, coming from the MCNP 6 nuclear data libraries. And the CGMF results refer to a standalone beta-version of the code not yet integrated in the MCNP 6 code and represent the prompt fission neutron and gamma-ray secondary particle emission only. Studying the models and their outputs prior to using them in a full transport simulation is important to identify correlations and trends in the output that the models are predicting. Once the behavior of the model is well established, then validation measurements will be needed to determine if and where deficiencies in the model exist.

### Average Quantities

The first quantities to compare between models are the average quantities such as the first moment of the neutron and gamma-ray multiplicity distributions,  $\bar{\nu}_N$  and  $\bar{\nu}_\gamma$ , respectively and the first moment of the neutron and gamma-ray energy spectrum,  $\langle E_N \rangle$  and  $\langle E_\gamma \rangle$ , respectively. An unexpected difference in these quantities could indicate a deficiency in the physics models implemented in the codes, and/or a problem in the model input parameters, such as the average total kinetic energy that mostly defined how much total excitation energy is in the fragments, and as a consequence, how many neutrons they can emit.

The average values listed in Table 1 are slightly difficult to compare due to the fact that the CGMF results are being computed outside of the MCNP 6 code unlike the FREYA results. However, because the only notable source of secondary neutron emission for the  $n(\text{thermal})+^{239}\text{Pu}$  reaction is from prompt fission events, the  $\bar{\nu}_N$  and  $\langle E_N \rangle$  values compare very nicely with each other as expected. The gamma-ray averages are more difficult to compare at the present time. It is known that the majority of the gamma-

Quantity	MCNP 6	FREYA	CGMF
$\bar{\nu}_N$	2.8725	2.8723	2.9764
$\bar{\nu}_\gamma$	2.0	7.2973	9.1797
$\langle E_N \rangle$ (MeV)	2.1034	2.0003	2.0327
$\langle E_\gamma \rangle$ (MeV)	0.9949	1.0327	0.7728

Table 1. The average multiplicity and energy of the neutrons and gamma rays for each code. Note the MCNP 6 and FREYA values include other sources of secondary particles such as the capture reaction gamma-ray emission whereas the CGMF standalone code is computing only prompt fission values.

ray production comes from the  $(n,f)$  fission reaction with most of the remaining production coming from the  $(n,\gamma)$  capture reaction. According to the ENDF/B-VII.1 nuclear data library [8] the capture reaction has a lower multiplicity and a higher average energy per gamma ray compared with the fission reaction. If the  $(n,\gamma)$  gamma-ray production reaction were combined with the CGMF results in Table 1, the results would be much closer to the FREYA/MCNP 6 results. The default behavior of MCNP 6 emits 2 gamma rays for each reaction, sampling the corresponding energies from the total gamma-ray production spectrum.

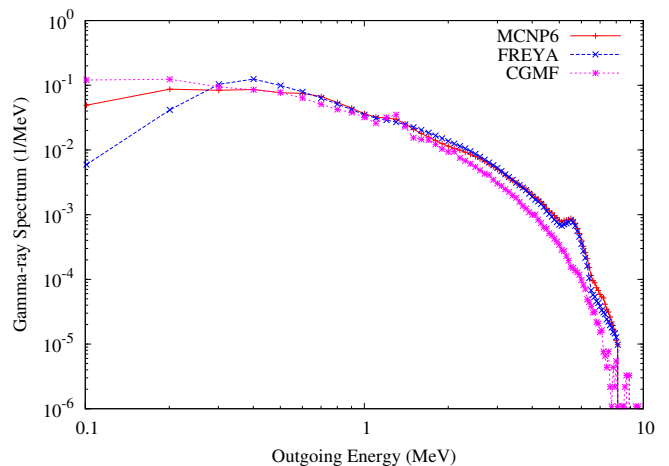


Fig. 1. The gamma-ray spectra of the  $n(\text{thermal})+^{239}\text{Pu}$  reaction calculated using MCNP 6, FREYA and CGMF. The MCNP 6 and FREYA results are total gamma-ray production spectra with the former being the default behavior from MCNP 6. The CGMF result is the prompt fission gamma-ray spectrum only computed from the standalone code.

The average outgoing energy spectrum of the gamma rays computed using the default MCNP 6 options and with FREYA turned on show good agreement above  $\sim 800$  keV, shown in Fig. 1. Below that, there are some noticeable differences where FREYA predicts a very rapid drop-off in

the low energy tail of the spectrum. Again, the major differences between the CGMF spectrum is the missing capture gamma-ray emission spectrum. The capture gamma-ray emission spectrum in the ENDF/B-VII.1 library has a peak near  $\sim 5.5$  MeV. The CGMF prompt fission gamma-ray spectrum combined with the ENDF/B-VII.1 capture gamma-ray emission spectrum would yield a spectrum similar to the MCNP 6/FREYA results in Fig. 1. Once CGMF is integrated into MCNP 6, these average values will be studied and compared again to verify the implementation has been done correctly.

### Neutron and Gamma-ray Correlations

The purpose for this work is not only to obtain good agreement with the neutron and gamma-ray average emission quantities in the nuclear data libraries but to also learn more about the fission process and to make better predictions when designing experiments. One of the benefits of using the multiplicity models is the very large amount of information that is available in the form of distributions like the multiplicity of neutrons and gamma rays,  $P(\nu_N)$  and  $P(\nu_\gamma)$ , respectively, and the individual average energy and energy spectrum for a given multiplicity.

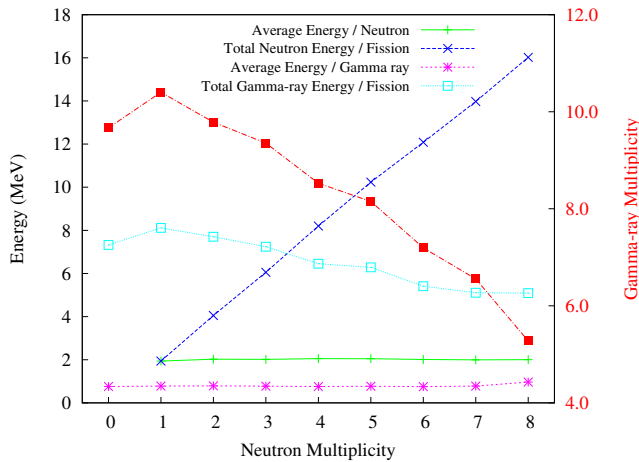


Fig. 2. The CGMF calculated total energy per fission event and average energy per particle for both neutron and gamma-ray emissions depending on the observed neutron multiplicity for the  $n(\text{thermal})+^{239}\text{Pu}$  prompt fission reaction. The gamma-ray multiplicity is anti-correlated to the neutron multiplicity as seen in the red curve corresponding to the second y-axis on the right.

In Fig. 2 several quantities are predicted by CGMF dependent on the neutron multiplicity that occurs for each event. First, the gamma-ray multiplicity is predicted to decrease from  $\sim 10$  for very low neutron multiplicity to  $\sim 5$  for very high neutron multiplicity. Both the neutron and

gamma-ray energy per emitted particle remains nearly constant while the total neutron energy per fission increases linearly and total gamma-ray energy per fission decreases with increasing neutron multiplicity. If it is possible to measure coincident neutrons and total gamma-ray energy in a complex detector setup, then this type of predicted dependence on the neutron multiplicity could be tested and possibly used in the detection of SNM. For example, coincidence experiments are being designed at the Los Alamos Neutron Science Center (LANSCE), making use of the DANCE 4-pi calorimeter along with a new compact neutron detector design, NEUANCE. This type of detector design will certainly help in the validation efforts for the multiplicity models and hopefully shed light on the predicted trends. CGMF predictions for the emission of prompt fission gamma rays depend sensitively on the initial angular momentum distributions in the fragments. At this point, those are modeled fairly crudely in the code, and future DANCE data should be able to guide the development of more advanced physics models, which may in turn modify the predictions presented here regarding neutron-gamma correlations.

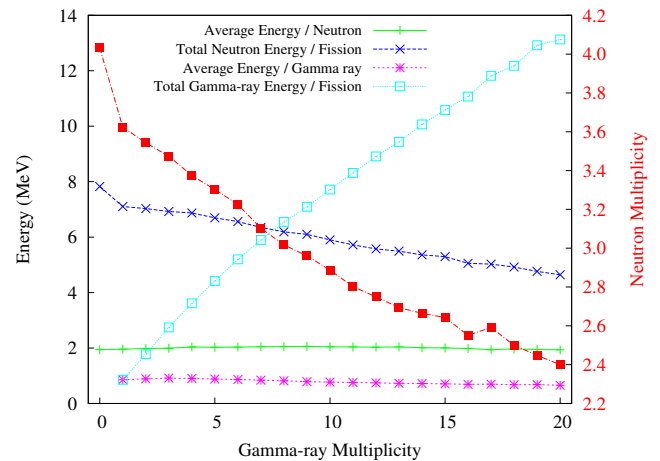


Fig. 3. The CGMF calculated total energy per fission event and average energy per particle for both neutron and gamma-ray emissions depending on the observed gamma-ray multiplicity for the  $n(\text{thermal})+^{239}\text{Pu}$  prompt fission reaction. Again, the neutron multiplicity is anti-correlated to the gamma-ray multiplicity as seen in the red curve corresponding to the second y-axis on the right.

By gating on the observed gamma-ray multiplicity for each event computed by CGMF, the same types of quantities displayed in Fig. 2 are shown in Fig. 3. Again, the neutron multiplicity decreases with increasing gamma-ray multiplicity. While the particle average energies remain nearly constant, the total neutron energy released in a fission event drops by 3-4 MeV and the total gamma-ray energy released

in a fission event increases almost linearly by  $\sim 10$  MeV for increasing gamma-ray multiplicity.

## CONCLUSIONS

By studying the fission multiplicity models, we are beginning to identify what kind of correlations and trends exist in the fission process. When the production version of CGMF is made available, the first goal will be to compare the results of a variety of MCNP 6 models to begin learning what SNM observables can be characterized for nonproliferation applications. Using the information provided by these complex models in FREYA and CGMF will hopefully help in distinguishing between SNM and non-fissile materials as well as identifying what kind of SNM is actually present and in what quantity. At the very least, adding physics improvements in the form of these high fidelity and rich fission models to the well-known MCNP 6 transport code will help in detector and experiment design for a large variety of applications. In the near future, this preliminary study will be extended and a more in-depth joint publication will be pursued by the FREYA, CGMF and MCNP 6 developers.

## ACKNOWLEDGMENTS

This work was supported by the Office of Defense Nuclear Nonproliferation Research & Development (DNN R&D), National Nuclear Security Administration, US Department of Energy.

## REFERENCES

1. MCNP6 Development Team, "Initial MCNP6 Release Overview - MCNP6 version 1.0," Los Alamos National Laboratory, LA-UR-13-22934 (2013).
2. J.T. Goorley, "MCNP6.1.1-Beta Release Notes," Los Alamos National Laboratory, LA-UR-14-24680 (2014).
3. J.M. Verbeke, C. Hagmann, and D. Wright, "Simulation of Neutron and Gamma Ray Emission from Fission and Photofission," Lawrence Livermore National Laboratory, UCRL-AR-228518 (2014).
4. R. Vogt and J. Randrup, "Event-by-event Study of Neutron Observables in Spontaneous and Thermal Fission," *Phys. Rev. C*, vol. 84, pp. 044612-1-14 (2011).
5. T. Kawano, P. Talou, M.B. Chadwick, and T. Watanabe, "Monte Carlo Simulation for Particle and  $\gamma$ -Ray Emissions in Statistical Hauser-Feshbach Model," *J. Nucl. Sci. Tech.*, **47** (5), 462-69 (2010).
6. B. Becker, P. Talou, T. Kawano, Y. Danon, and I. Stetcu, "Monte Carlo Hauser-Feshbach Predictions of Prompt Fission Gamma Rays - Application to  $n_{th} + {}^{235}\text{Pu}$  and  ${}^{252}\text{Cf}$  (sf)," *Phys. Rev. C*, **87**, 014617 (2013).
7. P. Talou, T. Kawano, I. Stetcu, R. Vogt, and J. Randrup, "Monte Carlo Predictions of Prompt Fission Neutrons and Photons: A Code Comparison," to appear in *Nucl. Data Sheets*.
8. M.B. Chadwick, M. Herman, P. Oblozinsky *et al.*, "ENDF/B-VII.1 Nuclear Data for Science and Technology: Cross Sections, Covariances, Fission Product Yields and Decay Data," *Nucl. Data Sheets*, **112**, 2887 (2011).